Effect of a Novel Phosphorus-Containing Compound on the Flame Retardancy and Thermal Degradation of Intumescent Flame Retardant Polypropylene

Shengqiang Zhang, Bin Li, Mo Lin, Qifei Li, Suliang Gao, Wei Yi

Heilongjiang Key Laboratory of Molecular Design and Preparation of Flame Retarded Materials, College of Science, Northeast Forestry University, Harbin 150040, People's Republic of China

Received 21 September 2010; accepted 25 February 2011
DOI 10.1002/app.34428
Published online 12 July 2011 in Wiley Online Library (wileyonlinelibrary.com).

ABSTRACT: A novel flame retardant, tetra(5,5-dimethyl-1,3- dioxaphosphorinanyl-2-oxy) neopentane (DOPNP), was synthesized successfully, and its structure was characterized by FT-IR, ^{1}H NMR, and ^{31}P NMR. The thermogravimetric analysis (TGA) results demonstrate that DOPNP showed a good char-forming ability. Its initial decomposition temperature was 236.4°C based on 1% mass loss, and its char residue was 41.2 wt % at 600°C, and 22.9 wt % at 800°C, respectively. The flame retardancy and thermal degradation behavior of novel intumescent flame-retardant polypropylene (IFR-PP) composites containing DOPNP were investigated using limiting oxygen index (LOI), UL-94 test, TGA, cone calorimeter (CONE) test, and scanning electron microscopy (SEM). The results demonstrate that DOPNP effectively raised LOI value of IFR-PP. When the loading of IFR was 30 wt %, LOI of IFR-PP reached 31.3%, and it passed UL-94 V-0. TGA results show that DOPNP made the thermal decomposition of IFR-PP take place in advance; reduced the thermal decomposition rate and raised the residual char amount. CONE results show that DOPNP could effectively decrease the heat release rate peak of IFR-PP. A continuous and compact char layer observed from the SEM further proved the flame retardance. © 2011 Wiley Periodicals, Inc. J Appl Polym Sci 122: 3430–3439, 2011

Key words: flame retardancy; cyclic phosphate ester; polypropylene; thermal degradation

INTRODUCTION

Many traditional halogen containing flame retardants are in a dilemma due to the strict requirement of less smoke and poison, this offers a good opportunity for the development of halogen-free flame retardants. Therefore, halogen-free flame retardants have been becoming one of the most promising flame retardants.[1–4] Non-halogen flame retardants are divided into inorganic and organic flame retardants. Generally, inorganic flame retardants have lower flame retardancy, and a high addition (more than 60 wt %) are needed, but they are less harmful.[5,6] Among organic flame retardants, intumescent flame retardants (IFRs) are well known as a new generation of flame retardants due to their merits, such as low smoke emission and toxic gases produced during burning, and antidripping property.[6–9] IFRs consist of three components: acid source [e.g., ammonium polyphosphate (APP)], carbonization source (e.g., pentaerythritol), and blowing agent (e.g., melamine). Besides, the synergistic agents (e.g., zeolite) have been used to enhance the flame retardancy of IFRs, and only the "components" reasonable match can promote the IFR systems to form a stable swell char layer.[10,11]

Generally, the halogen-free phosphorous flame retardants present the flame retardant mechanisms of condensed and gas phases in polymers, this depends on the type of phosphorus compounds, the chemical structure of polymers, and combustion conditions.[12,13] It has been reported that the P content of flame retardant is the most important factor affecting the flame retardancy,[14,15] and aliphatic phosphates are more desirable compounds to achieve high P content, and used as effective charring agents in IFRs. However, most of aliphatic structures of phosphates are easily hydrolytic.[16]

To achieve both high P content and hydro-stability, cyclic phosphate esters have been reported in the literatures.[17–20] Vothi et al. disclosed that a combination of cyclic structures with aromatic had good hydro-stability, high thermal stability, and good char-forming ability.[16] Hoang et al. synthesized a

Correspondence to: B. Li (libinzh62@163.com).
Contract grant sponsor: National Key Technology R and D Program; contract grant number: 2007BAE27B02.
Contract grant sponsor: Heilongjiang Technology R and D Program; contract grant number: TC10A0201.
Contract grant sponsor: NEFU Innovation Foundation for Postgraduates; contract grant number: gram 09.

aliphatic biscyclic phosphorus flame retardant (PBMP) with high P content (P% = 24.19) and good hydro-stability. However, its char-forming ability was low, only 6.8 wt % char residue at 700°C.[19]

In this article, we synthesized a new cyclic phosphate ester, tetra(5,5-dimethyl-1,3-dioxaphosphorinanyl-2-oxy) neopentane (DOPNP), which is hydrophobic in nature and shows high thermal stability and good char-forming ability due to the symmetrical structure. The molecular structure of DOPNP was characterized by FT-IR, ^{1}H NMR, and ^{31}P NMR spectroscopies. The flame retardancy and thermal behavior of a novel intumescent flame-retardant (IFR) system consisted of DOPNP, APP, melamine polyphosphate (MPP), and synergistic agent (4A zeolite) for PP were investigated.

EXPERIMENTAL

Materials

Polypropylene (PP) resin (homopolymer, melt flow rate: 3.5 g/10 min) was produced by Daqing Huake (Daqing, China). Ammonium polyphosphate (APP, GD-101, crystal form II, $n > 1500$, average particle size: 15 μm) was supplied by Zhejiang Longyou GD Chemical Industry Company (Longyou, China). Melamine polyphosphate (MPP, average particle size: 15 μm) was supplied by Jiangsu Zhenjiang Xingxing Flame Retardants (Zhenjiang, China).

All raw materials used in the synthesis of DOPNP included phosphorus oxychloride, neopentyl glycol, and pentaerythritol. Phosphorus oxychloride (analytical) was purchased from the Tianjin Guangfu Fine Chemical Research Institute (Tianjin, China), and neopentyl glycol (industrial) from the Shanghai Huanyu Chemical Reagent Factory (Shanghai, China). Pentaerythritol (industrial) was obtained from the Kermel Tianjin Chemical Reagent Company (Tianjin, China).

Synthesis of a novel phosphorus flame retardant (DOPNP)

The synthetic route of tetra(5,5-dimethyl-1,3-dioxaphosphorinanyl-2-oxy) neopentane (DOPNP) is shown in Scheme 1. The intermediate, 2-chloro-2-oxo-5,5-dimethyl-1,3,2-dioxaphosphorinane (DOPC) was first synthesized as the following process.

Neopentyl glycol (104.15 g, 1.0 mol) dispersed in dichloromethane (500 mL) was added in a dry, four-necked 1 L flask equipped with a mechanical stirrer, a thermometer, a reflux condenser, and a dropping funnel. The flask was immersed in an ice water bath. Phosphorus oxychloride (160.00 g, 1.05 mol) was added dropwise to the reaction flask over a period of 2 h, and the temperature was maintained at 0–5°C. After the addition, the reaction mixture was then allowed to warm up to room temperature and refluxed for 4 h until no HCl gas could be detected. The solvent was evaporated under a vacuum and the intermediate (DOPC) precipitated in distilled water, filtered, and dried for overnight to give a white powder (yield: 94%).

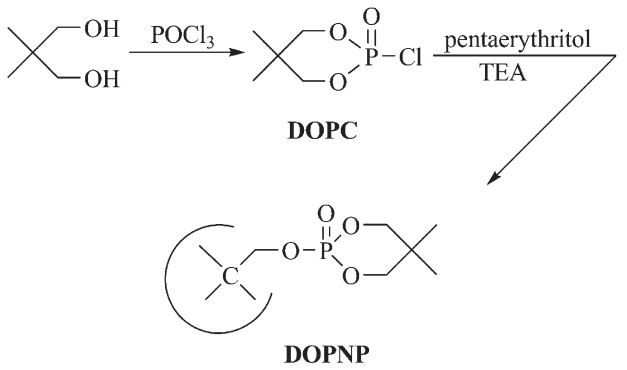

Scheme 1 Synthesis scheme of DOPNP.

DOPNP was prepared from the reaction of pentaerythritol with DOPC in the presence of acetonitrile. A mixture of pentaerythritol (34.04 g, 0.25 mol) and DOPC (193.79 g, 1.05 mol) dissolved in dry acetonitrile (500 mL) was placed into a dry, four-necked 1-L flask equipped with a mechanical stirrer, a thermometer, a reflux condenser, and a dropping funnel. Triethylamine (106.25 g, 1.05 mol) was added dropwise at 50°C over a period of 4 h. After the addition, the reaction temperature went up slowly to 80–90°C, refluxing for 48 h. After the removal of salt (Et_3N HCl) by filtering and evaporation of filtrate, the crude product was given; it was purified further by washing three times with aqueous solution of sodium bicarbonate and then washed with distilled water. After dried for overnight, the straw yellow solid (DOPNP) was obtained (yield: 65%).

Preparation of IFR-PP composites

Intumescent flame retardant polypropylene composites (IFR-PP) were prepared by the following procedure. First, All components shown in Table I were blended using a SHR high-speed mixer (Zhangjiagang, China) at below 80°C for 1 min, and the mixture was processed on a two-roll mill (Harbin Plastic Company, China) at a temperature range of 170–180°C for 10 min, then pressed on a curing machine at 170°C for 2 min to obtain various thick sheets, which were used to prepare various dimension sheets for all tests.

FT-IR, ^{1}H NMR, and ^{31}P NMR spectroscopies

FT-IR, ^{1}H NMR, and ^{31}P NMR were used to investigate the structure of DOPNP. ^{1}H NMR spectrum was obtained on an Infinity-plus 300 spectrometer

TABLE I
Effect of IFR Composition on Flame Retardance of PP

Sample	Composition of IFR-PP (wt %)						LOI (%)	UL-94 test	
	PP	DOPNP	APP	MPP	Zeolite 4A	Processing aid		Dripping	Rating
A	99.7	0	0	0	0	0.3	17.5	Yes	No rating
B	69.7	28.5	0	0	1.5	0.3	23.2	Yes	No rating
C	69.7	0	28.5	0	1.5	0.3	22.5	Yes	No rating
D	69.7	3.6	7.1	17.8	1.5	0.3	25.5	Yes	No rating
E	69.7	2.8	11.4	14.3	1.5	0.3	27.6	Yes	No rating
F	69.7	2.4	14.3	11.8	1.5	0.3	29.4	Yes	V-2
G	69.7	2.0	16.3	10.2	1.5	0.3	30.3	No	V-0
H	69.7	1.8	17.8	8.9	1.5	0.3	31.3	No	V-0
I	69.7	1.6	19.0	7.9	1.5	0.3	30.4	No	V-0
J	69.7	2.4	23.7	2.4	1.5	0.3	27.6	Yes	No rating
K	69.7	2.0	20.4	6.1	1.5	0.3	29.5	No	No rating
L	69.7	1.6	15.8	11.1	1.5	0.3	29.6	No	V-1
M	69.7	1.4	14.3	12.8	1.5	0.3	29.2	Yes	No rating

(Switzerland) at 300 MHz using $CDCl_3$ as a solvent and tetramethylsilane (TMS) as a reference. ^{31}P NMR spectrum was obtained on a superconducting NMR spectrometer of Bruker Avance DPX-400 (Switzerland) at 400 MHz using $CDCl_3$ as a solvent and tetramethylsilane (TMS) as a reference. The FT-IR spectra of DOPNP and DOPC were recorded with KBr powder using a Nicolet Avator 360 spectrometer (Wisconsin, USA).

Flame retardance tests

Limited oxygen index (LOI) values of all samples were obtained on a JF-3 oxygen index instrument (Jiangning, China) at room temperature with the dimension of 130 mm × 6.5 mm × 3 mm according to ASTM D2863-10. LOI is an important parameter for evaluating flame retardancy and flammability of polymeric materials in the same conditions. It denotes the lowest volume concentration of oxygen sustaining candle-like burning of materials in mixing gases of nitrogen and oxygen.

Vertical burning ratings of all samples were measured on a CZF-3 instrument produced by Jiangning Analysis Instrument Factory (Jiangning, China), with sample dimension of 130 mm × 13 mm × 3 mm according to ASTM D3801. UL-94 test results are classified by burning ratings V-0, V-1 or V-2.

Thermogravimetry analysis (TGA)

Thermogravimetry analysis (TGA) was performed on a Perkin–Elmer Pyris 1 Thermal Analyzer, (Massachusetts, USA) with platinum crucible sample holder. The samples were examined under flowing high-purity nitrogen of 50 mL min^{-1} at a constant heating rate of 10°C min^{-1} in the temperature range 50–800°C and the weight of all samples was kept within 3–5 mg.

Mechanical property tests

According to ASTM D638 and ASTM D790, tensile and flexural strength tests of 4.0 mm thick samples were carried out by Regeer computer controlled mechanical instrument (Shenzhen, China) with a crosshead speed of 15 and 2 mm min^{-1} at room temperature, respectively. Izod impact tests were performed by Notched Izod impact instrument (Chengde, China) according to ASTM D256. All the results reported were the average from five samples.

Cone calorimeter test

All CONE data were taken from a Cone Calorimeter [manufactured by Fire Testing Technology (West Sussex, UK)] at an incident heat flux of 50 kW m^{-2} according to ISO 5660-1 standard. The samples (100 mm × 100 mm × 3 mm) were laid on a horizontal sample holder.

Scanning electron microscopy (SEM)

The fractured surfaces and char residues of various samples were investigated by means of QUANTA-200, FEI scanning electron microscopy (Eindhoven, Netherlands). Cryogenic fractured surfaces were obtained by immersing the unbroken samples into liquid nitrogen for several minutes and breaking them with the tap of a hammer, which is called as brittle fracture. All the fracture surfaces and char residues were sputter-coated with gold layer before examination.

RESULTS AND DISCUSSION

Characterization of DOPNP

Figure 1 presents the FT-IR spectra of DOPC and DOPNP. From the spectrum of DOPNP, the

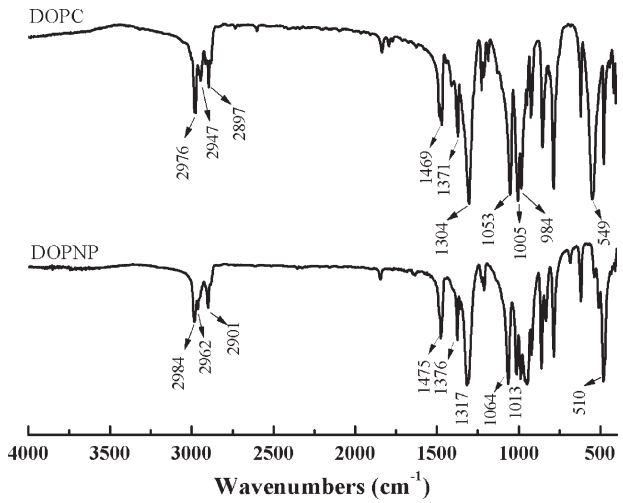

Figure 1 FT-IR spectra of DOPC and DOPNP.

absorption band at about 2900–2990 cm^{-1} was assigned to —CH_3 and —CH_2—, and the peak at 1376 cm^{-1} was assigned to —$C(CH_3)_2$— skeleton vibration from neopentyl glycol. Absorption of P=O was observed at about 1317 cm^{-1}. The peaks at 1064, 1013, and 988 cm^{-1} were associated with the stretching mode of P—O—C. The absorption at 861 cm^{-1} was assigned to the skeleton vibration of cyclic phosphates.[21,22] The strong absorption peak at 549 cm^{-1} from the intermediate (DOPC) was assigned to P—Cl. However, it disappeared completely in the spectrum of DOPNP, and the disappearance of the characteristic absorption band of O—H indicates that the final product was obtained successfully.

The ^{1}H NMR spectrum of DOPNP is shown in Figure 2. Two single specific chemical shifts at 0.93 and 1.30 ppm were attributed to the chemical shifts of —CH_3 protons (a) and (b), because the two —CH_3 groups are at both sides of a six-membered heterocyclic, and this results in unequivalent —CH_3 protons (a) and (b). The double peaks at 4.02 and 4.05 ppm were assigned to —CH_2— protons (e). The multiplet between 3.93 and 4.01 ppm and the double peaks at

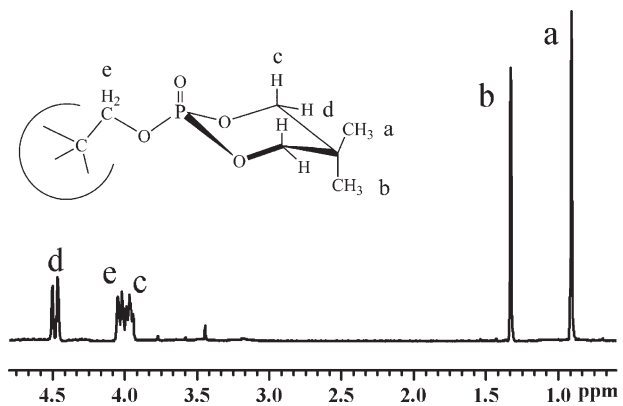

Figure 2 ^{1}H NMR of DOPNP in $CDCl_3$.

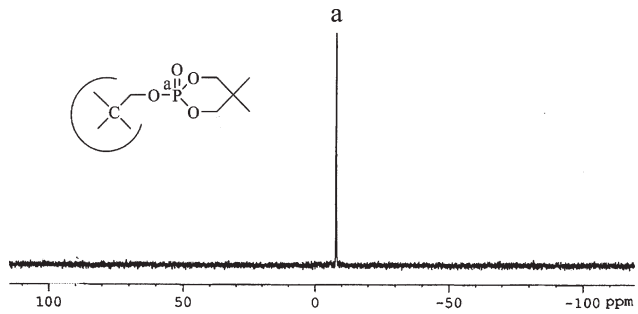

Figure 3 ^{31}P NMR of DOPNP in $CDCl_3$.

4.46 and 4.50 ppm were attributed to the —CH_2— protons (c) and (d) from the cyclic phosphonates, respectively,[16,23] that is because the —CH_2— protons (c) and (d) are at both sides of the six-membered heterocyclic (see in Fig. 2), and the different environment conditions lead to the two unequivalent protons (c) and (d). There was almost no specific chemical shift of the proton of —OH as presented in Figure 2. The ^{1}H NMR result is in agreement with the analysis on FT-IR of DOPNP. The structure of DOPNP is also confirmed by ^{31}P NMR spectrum shown in Figure 3. Only one sharp signal was appeared at −7.8 ppm. This result proved that the target product was synthesized successfully. The chemical structure of DOPNP is presented in Scheme 1, and the Kekulé model of DOPNP is shown in Figure 4.

Thermal degradation behavior of the DOPNP

Thermogravimetric analysis (TGA) is one of the most favorite techniques for evaluating thermal

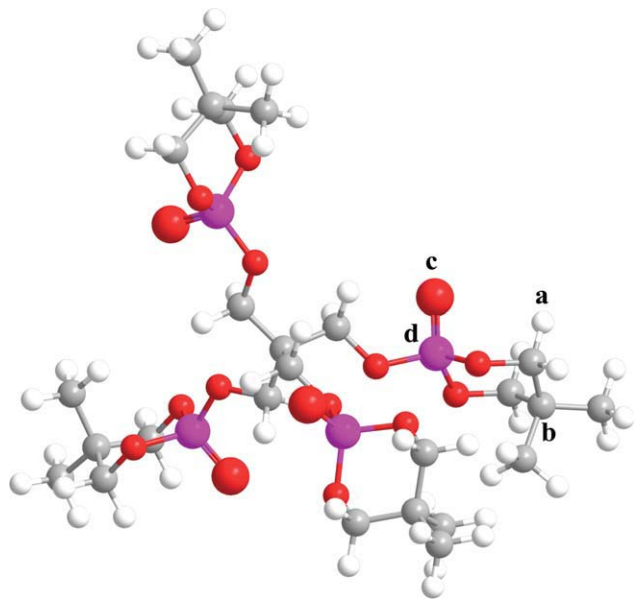

Figure 4 Kekulé model photograph of DOPNP: (a) H, (b) C, (c) O, and (d) P. [Color figure can be viewed in the online issue, which is available at wileyonlinelibrary.com.]

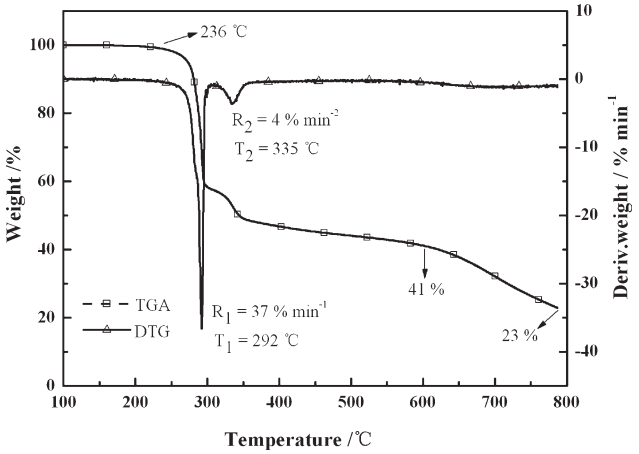

Figure 5 TGA and DTG curves of DOPNP.

degradation and stability of materials.[24–26] The TG data of DOPNP under pure nitrogen and the corresponding curves are presented in Figure 5. The initial decomposition temperature of DOPNP was 236°C, based on 1% mass loss, and the maximum temperature of thermal decomposition rate was 292°C. It is seen from the TGA curve that it underwent a two-step thermal degradation process. The first thermal degradation step occurred roughly from 220 to 310°C, the maximum rate of decomposition reached 37% min^{-1} and the mass loss was 42.4 wt % at 310°C. It is probably that the weaker P—O—C bonds of DOPNP broke down to form phosphoric acid or metaphosphoric acid.[27] Figure 6 shows the FT-IR spectra of DOPNP during the thermal degradation in the range of room temperature to 610°C. The intensities of the absorption bands at 2900–2990, 1469, and 1376 cm^{-1} decreased when the degradation temperature exceeded 290°C, and their absorption bands disappeared at higher temperature. These facts confirm that the cleavage of cyclic structure took place and the aliphatic —CH_2— groups eliminated.[28] The second thermal degradation step occurred from 310 to 360°C, and was assigned to a series of chemical reactions (crosslinking, dehydration and elimination) under the action of phosphoric acid and metaphosphoric acid. The absorption peak at nearby 3400 cm^{-1} appeared and became a broad absorption band increasingly, that was consistent with the first thermal degradation of DOPNP.[29] It is attributed to the formation of phosphoric acid groups during the decomposition of DOPNP. As can be seen from the Figure 6, the absorption peak at 1317 cm^{-1} (P=O) moved gradually to a lower wave number, while its intensity became weak increasingly from 310 to 500°C. From the data of Figure 5, the char residue of DOPNP was 41.2% at 600°C and 22.9% at 800°C, respectively. It showed a very effective charring ability.

Flame retardancy of the IFR-PP composites

A new intumescent flame retardant (IFR) consisted of DOPNP, APP, MPP, and 4A zeolite was used to obtain Intumescent flame-retardant polypropylene (IFR-PP). Of the components, DOPNP, APP, and MPP are mainly used as a charring agent, an acidic source and a blowing agent, respectively. Table I gives LOI values and UL-94 results of PP composites with 30 wt % loading of IFR or components. It was found that single component addition showed lower flame retardancy. The combination of them could obtain a satisfying flame retardant. The LOI values of IFR-PP systems rapidly increased and then decreased with the increase in the amount of APP, as the mass ratio of DOPNP to MPP was fixed at 1–5. When the mass ratio of DOPNP/APP/MPP was 1/10/5 (Sample H), the composite reached the highest value of 31.3% and UL-94 rating reached V-0 rating. Therefore, the optimal mass ratio of DOPNP to APP was 1 : 10. The addition of MPP in IFR also affected the flame retardancy of IFR-PP systems. From the data in Table I (Sample H, J–M), it was found that Sample H still presented the most effective flame retardancy in PP, that is, the best mass ratio of DOPNP/APP/MPP was 1/10/5.

Table II gives LOI and UL-94 data of IFR-PP systems with different addition of IFR (the mass ratio of DOPNP/APP/MPP was 1/10/5). It was found that LOI values of IFR-PP systems clearly increased with the increasing addition of IFR. When the addition of IFR in PP was 35 wt %, LOI value of IFR-PP system increased to 34.1%, and this system could pass UL-94 V-0 rating. However, none of IFR-PP systems could reach V-0 rating when the addition of IFR in PP was below 30 wt %.

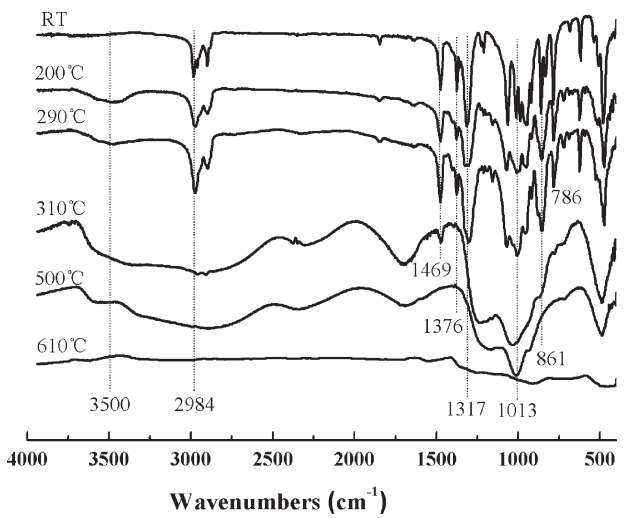

Figure 6 FT-IR spectra of DOPNP during the thermal degradation in the range of room temperature to 610°C.

TABLE II
The Flame Retardancy of IFR-PP Systems with Different Loadings of IFR

	Components of IFR-PP systems (wt %)				UL-94 test	
Sample	PP	IFR	Processing aid	LOI (%)	Flaming dripping	rating
A	99.7	0	0.3	17.5	Yes	No rating
B	89.7	10	0.3	21.1	Yes	No rating
C	84.7	15	0.3	22.8	Yes	No rating
D	79.7	20	0.3	24.9	Yes	No rating
E	74.7	25	0.3	28.6	Yes	V-2
F	69.7	30	0.3	31.3	No	V-0
G	64.7	35	0.3	34.1	No	V-0

Figure 7 gives the comparative analysis of LOI values of the IFR-PP systems with and without DOPNP. With the increasing addition of IFRs(-DOPNP-APP-MPP and APP-MPP) in PP, LOI values of IFR-PP composites (Curves a and b) increased. However, LOI values of DOPNP-APP-MPP-PP composite were clearly higher than these of APP-MPP-PP composite. For instance, when the loading of IFRs was 35 wt %, LOI values of DOPNP-APP-MPP-PP composite and APP-MPP-PP composite was 34.1 and 26.5%, respectively. Reogard2000, the commercial product of Great Lakes Chemical Corp., is based on phosphorus, nitrogen, and aluminosilicates. Compared with LOI value (26.7%) of IFR-PP with 25 wt % Reogard2000 reported by Vuillequez et al.,[28] the LOI value of DOPNP-APP-MPP-PP composite, 28.6%, is higher. Based on LOI values, the flame retardancy of DOPNP-APP-MPP is better than that of Reogard2000. According to UL-94 results, It was found all of APP-MPP-PP composites could not reach V-1 rating when the addition of APP-MPP composites in PP below 35 wt %. This is because APP-MPP-PP composites, lacking of a carbonization agent, can not form the effective protective char layer to achieve the heat insulation and the oxygen exclusion effect. Therefore, DOPNP effectively improves LOI value of IFR-PP, and DOPNP-APP-MPP is an effective intumescent flame-retardant for PP.

Thermal degradation behavior of IFRs and IFR-PP composites

Table III and Figure 8 give the thermal degradation data and TG curves of PP, DOPNP-APP-MPP, APP-MPP, DOPNP-APP-MPP-PP, and APP-MPP-PP in pure nitrogen. The initial decomposition temperature of DOPNP-APP-MPP and APP-MPP was 216 and 214°C, respectively, based on 1% mass loss. From Figure 8, DOPNP-APP-MPP underwent a three-step thermal degradation process at about 313, 355, and 434°C, which could be assigned to be dehydration, ammonia release, decomposition, crosslinking, and charring processes of IFRs. The first thermal degradation step of DOPNP-APP-MPP occurred roughly from 220 to 320°C, and its maximum rate of decomposition was 2.2% min^{-1}. The second thermal degradation step took place at between 320 and 380°C, and it was probably corresponding to chemical reactions of dehydration and release of ammonia. Compared with APP-MPP (3.1% min^{-1}), its maximum decomposition rate was lower, reduced to 1.5% min^{-1}. The third thermal degradation step occurred roughly from about 380 to 520°C, which could be assigned to the decomposition of phosphates, and its maximum decomposition rate (2.5% min^{-1}) was almost the same with APP-MPP (2.3% min^{-1}). The char residue of DOPNP-APP-MPP was 55.1 wt % at 600°C and 47.5 wt % at 800°C, and that of APP-MPP was 56.1 wt % at 600°C and 43.5 wt % at 800°C. The results show that DOPNP-APP-MPP displays a good charring ability at the high temperature.

From the data of curve a shown in Figure 8, the thermal degradation behavior of PP showed only one peak of PP backbone decomposition at 472°C and the maximum decomposition rate was very fast

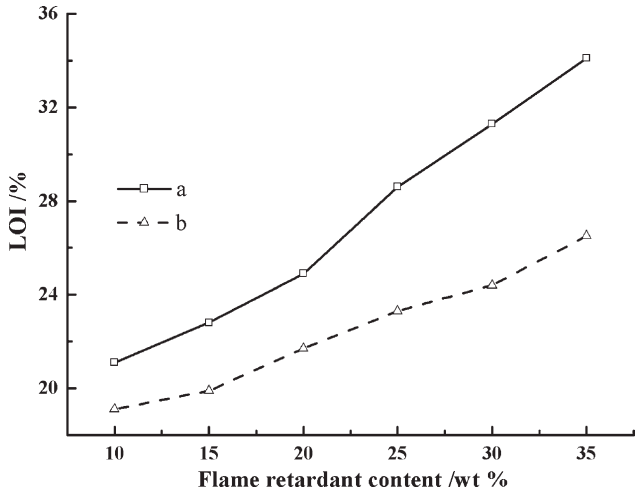

Figure 7 LOI values of the IFR-PP systems with and without DOPNP: (a) DOPNP-APP-MPP-PP and (b) APP-MPP-PP.

TABLE III
Thermal Degradation Data of Samples by TG

Sample	$T_{initial}$ (°C)	R_{1peak}/T_{1peak} (% min^{-1}/°C)	R_{2peak}/T_{2peak} (% min^{-1}/°C)	R_{3peak}/T_{3peak} (% min^{-1}/°C)	Char residue (%) 600°C	800°C
PP	330.2	27.5/471.6	–	–	0.7	0
DOPNP-APP-MPP	215.5	2.2/312.8	1.5/355.1	2.5/433.5	55.1	47.5
APP-MPP	213.7	3.1/358.5	2.3/429.7	–	56.1	43.5
DOPNP-APP-MPP-PP	270.7	0.6/295.8	1.5/400.2	21.8/483.1	16.1	15.6
APP-MPP-PP	287.5	2.1/396.4	26.9/489.4	–	15.5	13.3

(27.5% min^{-1}). There was almost no char residue remained at over 600°C. From curves d, e in Figure 8 and the data of Table III, it is seen that the initial decomposition temperature of DOPNP-APP-MPP-PP composite was ahead of over 50°C relative to pure PP, whereas the maximum thermal decomposition temperature was delayed over 10°C. We found that the initial decomposition temperature of APP-MPP-PP composite was 287°C and its char residue was 13.3 wt % at 800°C. However, the initial decomposition temperature of DOPNP-APP-MPP-PP composite was 271°C, ahead of about 20°C relative to APP-MPP-PP composite, and its char residue was 15.6 wt % at 800°C, that is because DOPNP could decompose at the low temperature, and present a good charring ability.

Cone calorimeter study

Cone calorimetry is one of the most effective bench-scale methods for evaluating the flammability of materials. It can provide a wealth of information on the combustion behavior, and give a measure of the size of the fire.[30,31] The heat release rate (HRR) is presented in Figure 9, which is recognized to be the most important parameter to measure the developing and spreading of fire.[32,33] From Figure 9, the pure PP (curve a in Fig. 9) burned very fast after ignition and a sharp HRR peak (1180.5 kW m^{-2}) appeared at 170 s, while the HRR peak value of the DOPNP-APP-MPP-PP composite (Sample H in Table I) obviously reduced to 294.0 kW m^{-2} and its ignition time was lower than PP due to the flame retardant additive lead to earlier char formation. Compared with the APP-MPP-PP composite, the DOPNP-APP-MPP-PP composite showed a better flame retardancy. This result is in an agreement with LOI and UL-94 results. The total heat release (THR) curves of the composites are given in Figure 10. The maximum THR value of DOPNP-APP-MPP-PP composite (3220.7 MJ m^{-2} kg^{-1}) decreased obviously compared to pure PP (4001.5 MJ m^{-2} kg^{-1}), but almost no change relative to APP-MPP-PP composite (3205.2 MJ m^{-2} kg^{-1}). However, the time of DOPNP-APP-MPP-PP composite for reaching the maximum THR was prolonged. The mass curves of pure PP, DOPNP-APP-MPP-PP composite, and APP-MPP-PP composite are presented in Figure 11. The tendency of their mass loss is similar to that of HRR. But the decomposition of DOPNP-APP-MPP-PP composite became slow, and its char residue content enhanced. These results further demonstrate that the

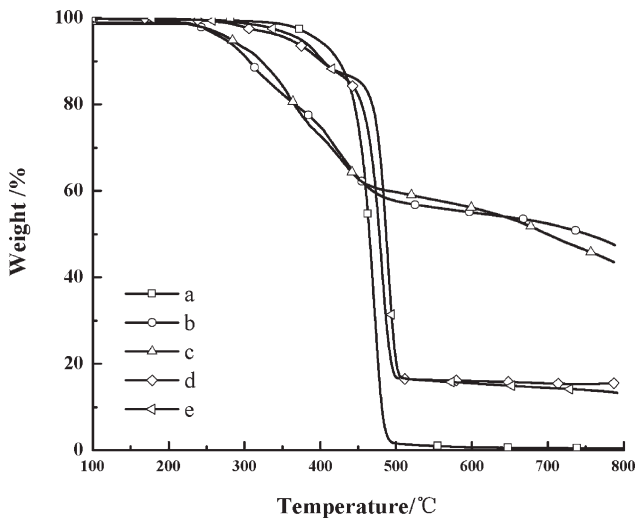

Figure 8 Comparison of TG curves of various samples: (a) PP, (b) DOPNP-APP-MPP, (c) MPP-APP, (d) DOPNP-APP-MPP-PP, and (e) APP-MPP-PP.

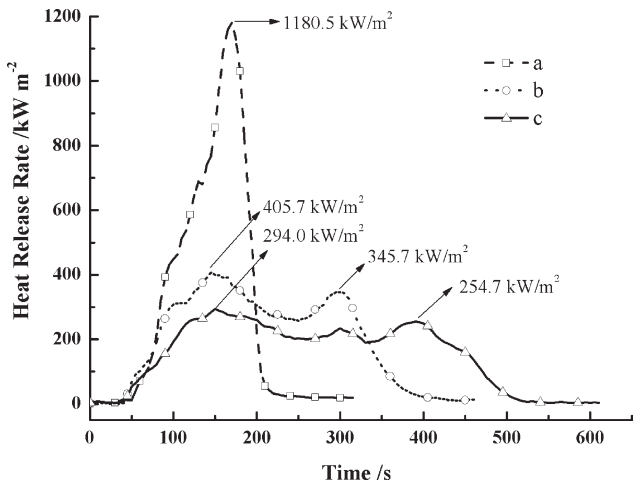

Figure 9 Heat release rate curves of samples: (a) PP, (b) APP-MPP-PP and (c) DOPNP-APP-MPP-PP.

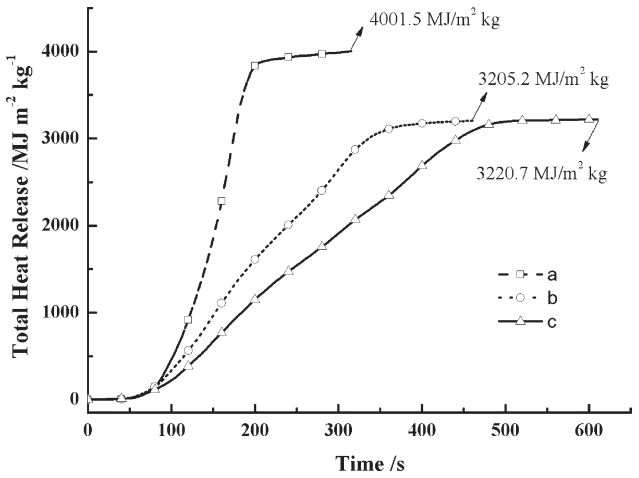

Figure 10 Total heat release curves of samples: (a) PP, (b) APP-MPP-PP, and (c) DOPNP-APP-MPP-PP.

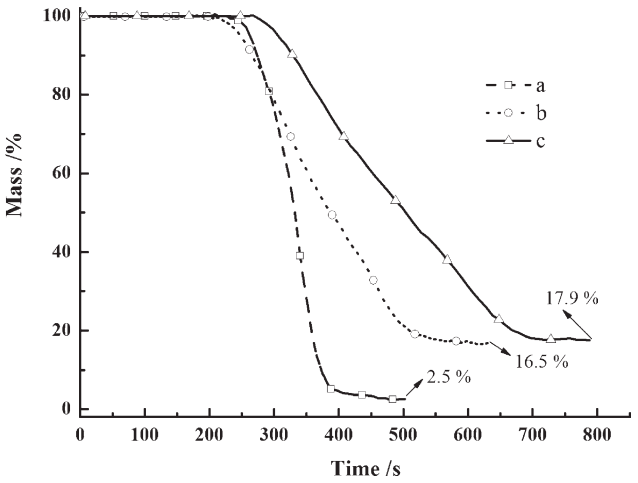

Figure 11 Mass curves of samples: (a) PP, (b) APP-MPP-PP, and (c) DOPNP-APP-MPP-PP.

IFR-PP system using DOPNP as carbonization agent had excellent flame retardancy.

Mechanical properties

Tables IV and V give the effect of IFR loadings on the mechanical properties of IFR-PP composites. Compared with pure PP, flexural strength of both DOPNP-APP-MPP-PP and APP-MPP-PP composites slowly increased, whereas tensile strength and notched Izod impact strength obviously decreased. However, at the high loadings of IFR, tensile strength and notched Izod impact strength of DOPNP-APP-MPP-PP composite were better than these of APP-MPP-PP composite. For example, when the loading of IFR was 30 wt %, flexural strength, tensile strength and notched izod impact strength of DOPNP-APP-MPP-PP composite were 42.9 MPa, 25.4 MPa, and 2.7 kJ m^{-2}, while 41.1 MPa, 22.1 MPa, and 2.3 kJ m^{-2} for APP-MPP-PP composite, respectively. This is caused by a certain DOPNP addition. This result is attributed to a large quantity of methyl groups in DOPNP, which probably increase the compatibility of PP and DOPNP-APP-MPP.

SEM analysis

The SEM micrographs of fractured surfaces of IFR-PP systems with and without DOPNP are showed in Figure 12. Compared Figure 12(a) with 12(b), it was found that the IFR with DOPNP showed better compatibility in PP than the one without DOPNP, which was in agreement with the results of mechanical properties at the high loading.

Figure 13 shows SEM micrographs of the char residues of IFR-PP systems with and without DOPNP to elucidate the relationship between the microstructure of protective char layer and flame retardancy. The char residues were collected from the limiting oxygen index tests of IFR-PP systems. It was found that the char layer's outer surface of APP-MPP-PP composite [Fig. 13(b)] was porous, which could not effectively hinder the thermal degradation of underlying PP and the release of combustible volatiles. However, when DOPNP was added in the composite, its char residue [Fig. 13(a)] was almost no holes and had a continuous, compact intumescent char layer, which could effectively restrict mass and the heat transfer from interior to outer.[34–36] This result

TABLE IV
Mechanical Properties of IFR-PP Systems with Different Loadings of IFR with DOPNP

	Composition of IFR-PP Systems (wt %)			Mechanical properties		
Sample	PP	DOPNP-APP-MPP	Processing aid	Tensile strength (MPa)	Flexural strength (MPa)	Izod impact strength (kJ m^{-2})
A	99.7	0	0.3	32.2 ± 0.3	38.1 ± 0.3	3.8 ± 0.2
B	89.7	10	0.3	29.3 ± 0.2	40.4 ± 0.5	3.6 ± 0.3
C	84.7	15	0.3	27.5 ± 0.5	41.4 ± 0.4	3.2 ± 0.1
D	79.7	20	0.3	27.0 ± 0.4	42.3 ± 0.3	3.3 ± 0.2
E	74.7	25	0.3	25.3 ± 0.2	42.6 ± 0.5	2.8 ± 0.3
F	69.7	30	0.3	25.4 ± 0.3	42.9 ± 0.4	2.7 ± 0.2
G	64.7	35	0.3	25.4 ± 0.4	41.7 ± 0.5	2.1 ± 0.1

TABLE V
Mechanical Properties of IFR-PP Systems with Different Loadings of IFR Without DOPNP

	Composition of IFR-PP Systems (wt %)			Mechanical properties		
Sample	PP	APP-MPP	Processing aid	Tensile strength (MPa)	Flexural strength (MPa)	Izod impact strength (kJ m^{-2})
A	99.7	0	0.3	32.2 ± 0.3	38.1 ± 0.1	3.8 ± 0.2
B	89.7	10	0.3	29.1 ± 0.2	42.1 ± 0.6	3.6 ± 0.3
C	84.7	15	0.3	27.2 ± 0.5	41.0 ± 0.5	3.0 ± 0.2
D	79.7	20	0.3	25.3 ± 0.3	41.8 ± 0.5	3.0 ± 0.1
E	74.7	25	0.3	25.1 ± 0.2	42.4 ± 0.3	2.5 ± 0.2
F	69.7	30	0.3	22.1 ± 0.4	41.1 ± 0.5	2.3 ± 0.3
G	64.7	35	0.3	20.1 ± 0.5	40.4 ± 0.3	1.9 ± 0.1

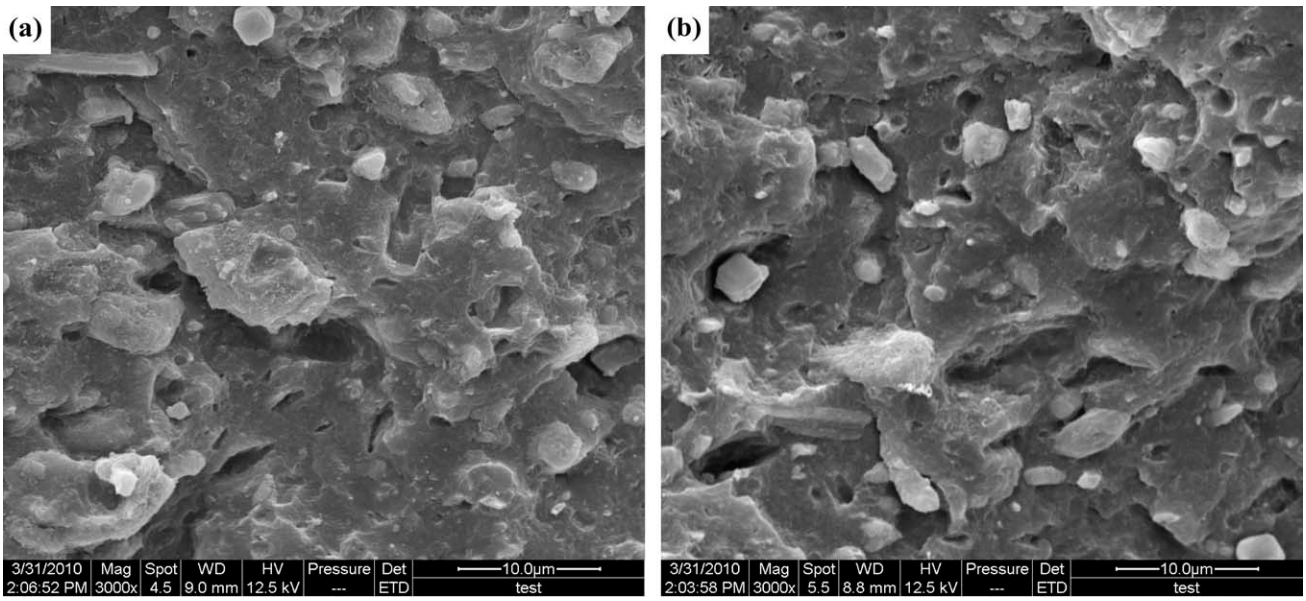

Figure 12 SEM photos of the fractured surface of samples (×3000): (a) DOPNP-APP-MPP-PP and (b) APP-MPP-PP.

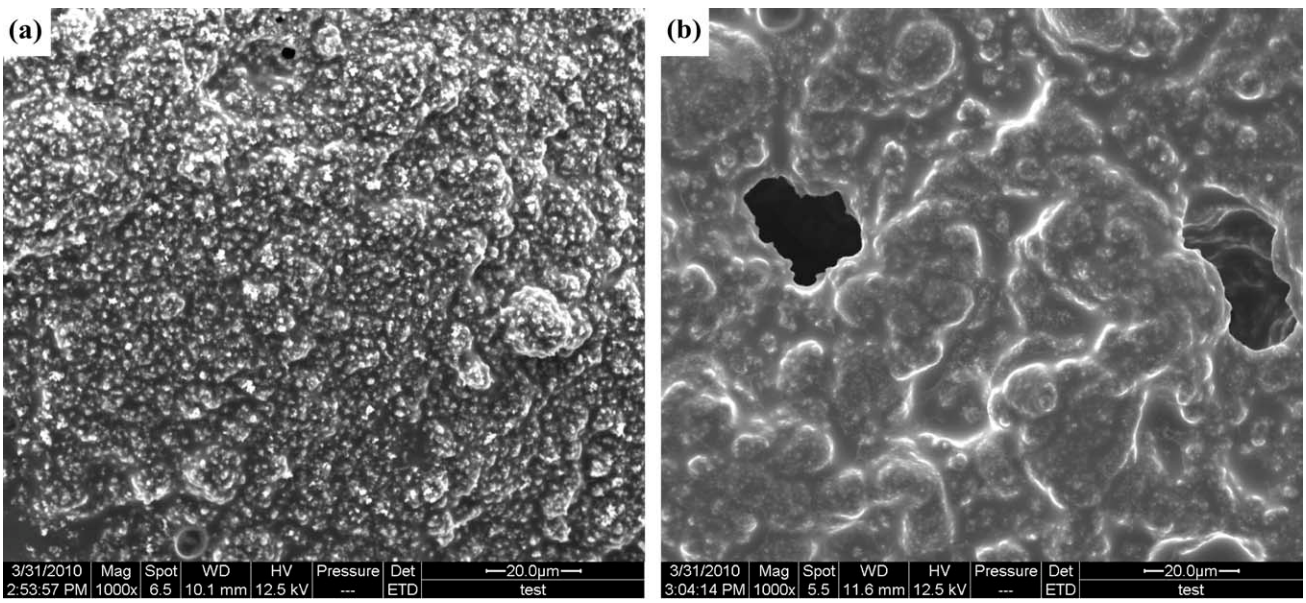

Figure 13 SEM photos of the surface of the burnt char residue (×1000): (a) DOPNP-APP-MPP-PP and (b) APP-MPP-PP.

also proves that DOPNP-APP-MPP composite is an effective Intumescent flame-retardant for PP.

CONCLUSIONS

A novel charring agent of DOPNP was synthesized successfully and its chemical structure was confirmed by FT-IR, ^{1}H NMR, and ^{31}P NMR. The results of TG indicate that DOPNP showed a good charring ability. The intumescent flame retardant (IFR) using DOPNP, as carbonization agent, showed better flame retardancy for PP, and synergistic effects among DOPNP, APP and MPP was crucial to fully exert the flame retardance of the IFR system. The optimal flame retardant formulation was DOPNP/APP/MPP = 1/10/5, at which the LOI value was 31.3% and it passed UL-94 V-0 rating, as the addition of IFR was 30 wt %. Based on the heat release rate (HRR) peak, total heat release (THR), and mass loss of IFR-PP from the cone calorimeter, it was further shown that the IFR with DOPNP presented more effective flame retardancy for PP. SEM micrographs and mechanical property results also proved that DOPNP showed better compatibility of IFR and PP matrix.

References

1. Wang, L. S.; Kang, H. B.; Wang, S. B.; Liu, Y.; Wang, R. Fluid Phase Equilibr 2007, 258, 99.
2. Lu, S. Y.; Hamerton, I. Prog Polym Sci 2002, 27, 1661.
3. Siriviriyanun, A.; O'Rear, E. A.; Yanumet, N. J Appl Polym Sci 2008, 109, 3859.
4. Spontón, M.; Lligadas, G.; Ronda, J. C.; Galià, M.; Cádiz, V. Polym Degrad Stab 2009, 94, 1693.
5. Peng, H. Q.; Zhou, Q.; Wang, D. Y.; Chen, L.; Wang, Y. Z. J Ind Eng Chem 2008, 14, 589.
6. Wang, Z. Z.; Qu, B. J.; Fan, W. C.; Huang, P. J Appl Polym Sci 2001, 81, 206.
7. Li, B.; Jia, H.; Guan, L. M.; Bing, B. C.; Dai, J. F. J Appl Polym Sci 2009, 114, 3626.
8. Ke, C. H.; Li, J.; Fang, K. Y.; Zhu, Q. L.; Zhu, J.; Yan, Q.; Wang, Y. Z. Polym Degrad Stab 2010, 95, 763.
9. Xie, F.; Wang, Y. Z.; Yang, B.; Liu, Y. A. Macromol Mater Eng 2006, 19, 247.
10. Li, B.; Xu, M. J Polym Degrad Stab 2006, 91, 1380.
11. Nguyen, C.; Kim, J. Polym Degrad Stab 2008, 93, 1037.
12. Morgan, A. B.; Tour, J. M. J Appl Polym Sci 1999, 73, 703.
13. Youssef, B.; Mortaigne, B.; Soulard, M.; Saiter, J. M. J Therm Anal Cal 2007, 90, 489.
14. Weil, E. D.; Zhu, W.; Patel, N.; Mukhopadhyay, S. M. Polym Degrad Stab 1996, 54, 125.
15. Price, D.; Cunliffe, L. K.; Bullett, K. J.; Hull, T. R.; Milnes, G. J.; Ebdon, J. R.; Hunt, B. J.; Joseph, P. Polym Degrad Stab 2007, 92, 1101.
16. Vothi, H.; Nguyen, C.; Lee, K.; Kim, J. Polym Degrad Stab 2010, 95, 1092.
17. Hoang, D. Q.; Kim, J.; Jang, B. N. Polym Degrad Stab 2008, 93, 2042.
18. Zhang, Q. B.; Xing, H. T.; Sun, C. Y.; Xing, H. W.; Jiang, D. W.; Qin, L. L. J Appl Polym Sci 2010, 115, 2170.
19. Hong, D. Q.; Kim, J. Polym Degrad Stab 2008, 93, 36.
20. Song, P. G.; Fang, Z. P.; Tong, L. F.; Jin, Y. M.; Lu, F. Z. J Anal Appl Pyrol 2008, 82, 286.
21. Song, P. G.; Tong, L. F.; Fang, Z. P. J Appl Polym Sci 2008, 110, 616.
22. Li, Q.; Jiang, P. K.; Wei, P. Polym Eng Sci 2006, 46, 344.
23. Wang, D. Y.; Cai, X. X.; Qu, M. H.; Liu, Y.; Wang, J. S.; Wang, Y. Z. Polym Degrad Stab 2008, 93, 2186.
24. Dai, J. F.; Li, B. J. Appl Polym Sci 2010, 116, 2157.
25. Wang, Z. Z.; Lv, P.; Hu, Y.; Hu, K. L. J Anal Appl Pyrol 2009, 86, 207.
26. Liu, Y.; Wang, Q. J Appl Polym Sci 2008, 107, 14.
27. Lu, L. G.; Wang, D. W.; Dong, X. L.; Yang, S. S.; Xu, X. N.; Wang, X. B.; Zhang, Y.; Yu, B. G.; Gao, W. Y. Acta Chem Sin 2008, 66, 2489.
28. Vuillequez, A.; Lebrun, M.; Ion, R. M.; Youssef, B. Macromol Symp 2010, 290, 146.
29. Lv, P.; Wang, Z. Z.; Hu, K. L.; Fan, W. C. Polym Degrad Stab 2005, 90, 523.
30. Price, D.; Bullett, K. J.; Cunliffe, L. K.; Hull, T. R.; Milnes, G. J.; Ebdon, J. R.; Hunt, B. J.; Joseph, P. Polym Degrad Stab 2005, 88, 74.
31. Fontaine, G.; Bourbigot, S.; Duquesne, S. Polym Degrad Stab 2008, 93, 68.
32. Redfern, J. Mater World 1996, 4, 73.
33. Wu, Z. P.; Shu, W. Y.; Hu, Y. C. J Appl Polym Sci 2007, 103, 3667.
34. Ma, Z. L.; Gao, J. G.; Bai, L. G. J Appl Polym Sci 2004, 92, 1388.
35. Nie, S. B.; Hu, Y.; Song, L.; He, S. Q.; Yang, D. D. Polym Adv Technol 2008, 19, 489.
36. Liu, M. F.; Liu, Y.; Wang, Q. Macromol Mater Eng 2007, 292, 206.